since 1961

BALTICA Volume 37 Number 12 December 2024: 80–99
https://doi.org/10.59879/tWHTQ

Hydrocarbon Reservoir Suitability of Permian Bewah Limestone, Eastern Peninsular Malaysia: A Thin-Section Pore Imaging Study

Muhd Nur Ismail Abdul Rahman[1,2,3*], Mazni Mustapha[1], Dony Adriansyah Nazaruddin[1,2], Muhammad Afiq Md Ali[1,2], Nor Bakhiah Baharim[1,2]

[1]Faculty of Science and Marine Environment, Universiti Malaysia Terengganu, 21030 Kuala Nerus Terengganu
[2]Research Outreach Collaboration Knowledge Research Interest Group (ROCK) Faculty of Science and Marine Environment, Universiti Malaysia Terengganu, 21030 Kuala Nerus Terengganu
[3]Aqua Heritage Research Interest Group Faculty of Science and Marine Environment, Universiti Malaysia Terengganu, 21030 Kuala Nerus Terengganu

[*]Corresponding author: nur.ismail@umt.edu.my

Abstract. This article presents the findings of a suitability assessment for hydrocarbon reservoir analogues using pore imaging techniques on selected limestone samples. The study focuses on the Bewah Limestone in the eastern part of Peninsular Malaysia, which dates back to the Permian period. The Bewah Limestone is classified as a metasediment and consists of mudstone, dolomite, and crystallized limestone. Thin polished sections from ten limestone samples were analyzed, and these were successfully categorized as mudstone, wackestone, packstone, dolomite, and rudstone. The samples were then analyzed using ImageJ software to quantify porosity, with porosity levels determined by applying thresholds to grayscale images. Porosity results varied across the samples, ranging from poor to good, based on the hydrocarbon reservoir quality index. The highest recorded porosity was 20.24%, classified as good, while fair porosity ranged from 11.6% to 11.93%. Most samples exhibited poor porosity, ranging from 6.10% to 9.52%. Pore connectivity was assessed using different threshold levels to better understand fluid flow. The results suggest that the Bewah Limestone samples have the potential to store and trap hydrocarbon fluids, indicating their suitability as hydrocarbon reservoir analogues.
Keywords: Bewah Limestone, ImageJ, Porosity, hydrocarbon reservoir analogue

INTRODUCTION

The Bewah Limestone, located at Kenyir Lake in Hulu Terengganu (Figure 1A), is one of the key carbonate rock formations in Terengganu State. It features a unique, isolated karst morphology that sets it apart from other limestone distributions in Malaysia. This remarkable formation, which is over 270 million years old, has been designated a national geopark in recognition of its preserved geological heritage (Figure 1B). Situated in the Eastern Belt near

BALTICA Volume 37 Number 12 December 2024: 80–99
https://doi.org/10.59879/tWHTQ

Kenyir Lake, it consists of various carbonate rocks, including dolomite and calcite, that formed during the Permian period (Zahidin et al., 2017; Rahman et al., 2023). The limestone is primarily composed of calcite, lime mud, and dolomite (Sharoum et al., 2015). Fossils of bivalves, crinoids, bryozoans, cephalopods, and foraminifera have also been discovered within the Bewah Limestone (Sharoum et al., 2015). In addition, ancient human remains, estimated to be around 16,000 years old, were uncovered during an expedition in 2009 in Bewah Cave (Zahidin et al., 2017).

Carbonate rocks, on the other hand, play a critical role in the oil and gas industry as hydrocarbon reservoirs, hosting substantial hydrocarbon reserves worldwide. Carbonate rocks such as limestone and dolomite form in marine environments, where calcium carbonate accumulates from marine organisms and precipitation from seawater (Xia et al., 2019; Janjuhah et al., 2021; Machel, 2005). Over time, these rocks undergo diagenetic processes—transformations that occur after deposition and burial. Diagenesis significantly influences the reservoir properties of carbonate rocks and includes processes like compaction, cementation, dissolution, recrystallization, and the development of secondary porosity (Morton-Thompson & Woods, 1993). Understanding diagenetic evidence is crucial for tracing the history of a carbonate reservoir, as it involves analyzing these processes and their impact on reservoir quality through petrographic analysis. Reservoir analogues—existing oil and gas fields with geological and petrophysical characteristics similar to target reservoirs—provide valuable insights. Limestone reservoir analogues, in particular, are vital in the exploration and production of hydrocarbons from limestone formations.

Advances in digital imaging and computer software have revolutionized petrographic analysis, enabling a wide range of image analysis techniques (Beggan & Hamilton, 2010). Textures can now be digitized, allowing for rapid measurement of features like grain or crystal size, shape, and sorting (Higgins & Roberge, 2007; Jerram et al., 2009). Computer models can generate virtual textures with known 3D properties, which serve as benchmarks for analyzing natural samples (Jerram, 2001; Jerram & Cheadle, 2000; Hersum & Marsh, 2007). Grove and Jerram (2011) explored the use of image processing, specifically the jPOR/ImageJ method, to assess porosity. Numerous studies have employed ImageJ for porosity analysis, including investigating the relationship between porosity and fluid viscosity (Stevens, 2016), comparing porosity values for petrophysical analysis (Viet, 2014), and comparing porosity distribution obtained from ImageJ with scanning electron microscopy (SEM) (Rine et al., 2013; Saraf et al., 2019), as well as quantifying porosity and modeling with ImageJ (Pal et al., 2022). However, few researchers have applied ImageJ to study hydrocarbon reservoir analogues. Thus, this study aims to use ImageJ software to quantify porosity in Permian limestone as an analogue for evaluating the suitability of hydrocarbon reservoirs.

BALTICA Volume 37 Number 12 December 2024: 80–99
https://doi.org/10.59879/tWHTQ

GENERAL GEOLOGY

The Eastern Belt of Malaysia refers to a geological region located on the eastern side of Peninsular Malaysia. It encompasses parts of the states of Kelantan, Terengganu, and Pahang. The geology of the Eastern Belt is characterized by a diverse range of rock formations and tectonic events that have shaped the landscape over millions of years. The strong tectonic activity in Peninsular Malaysia in the Late Triassic (237 Ma), especially in the Western, Central, and Eastern Orogenic Belts, significantly altered every region of the peninsula (Metcalfe (1988); Khoo and Tan (1983)) (Figure 2 (B)). When this tectonic activity first began, the Sibumasu terrane split off from Gondwanaland and collided with the Indo-China/East Malaya terrane, creating the Bentong-Raub Suture zone (Metcalfe, 2011).

Kenyir Lake is located on the East Malaya Blocks, also known as the western margin of the Indochina Terrane (Sukhotai back-arc). According to Roselee et al. (2018), despite the presence of plutonic and volcanic rocks, sedimentary formations predominate in the region. According to Metcalfe (2011), the volcanic rocks formed during the Late Permian to Early Triassic period as the Paleo-Tethys Ocean subducted beneath the East Malaya Block. Kenyir Lake region and other nearby sedimentary rocks, such as hornfels and quartzite, have undergone metamorphic rock formation as a result of granite intrusion. The sedimentary and igneous rock units that make up Kenyir Lake connect the entire lake area. The Sungai Kerbat Shale, Sungai Petang Sandstone, Bewah Limestone, Metong Conglomerate, and Gagau Group are the sedimentary rock units (Chung et al., 2017). The oldest rocks, Sungai Kerbat Shale and Sungai Petang Sandstone, which were deposited in a marine environment during the Late Carboniferous, make up the geology of Kenyir Lake (Rahman et al., 2023).

Due to the buildup of shells and benthic organism replacement, the carbonate rock revealed in Kenyir Lake, known as the Bewah Limestone, was deposited during the Early Permian era. It is thought that carbonate rock continued to form during the Permian period. The age of the Bewah Limestone is estimated to be Permian age. This age determination is based on the analysis of benthic foraminifera assemblages found within the formation. The Gua Musang Formation may be a component of the Bewah Limestone, which is situated close to the Gua Musang Formation and south of Kenyir Lake in Kelantan. The Bewah Limestone undergone low to moderate metamorphism process during Late Triassic igneous intrusion (Ali et al., 2006). Due to dolomite and some of the limestone experience crystalline. Additionally, this sequence is quite similar to the greater carbonate buildup in Peninsular Malaysia, which was exposed after major tectonic emplacement during the Late Triassic (Figure 2 (A).

BALTICA Volume 37 Number 12 December 2024: 80–99
https://doi.org/10.59879/tWHTQ

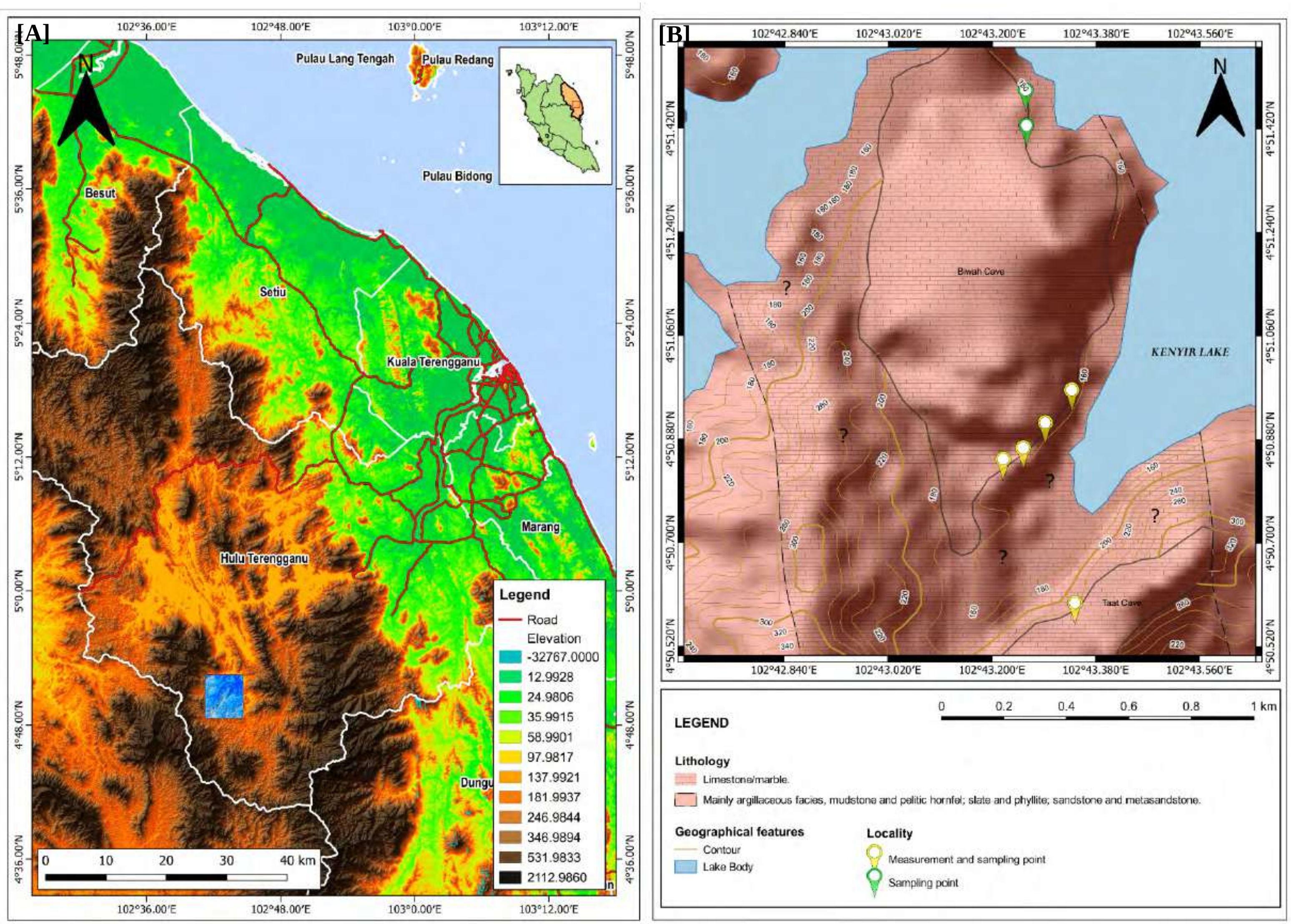

Figure 1. [A] Map of Terengganu showing the general location of the study area (blue box). [B] Detailed view of the study area with specific sampling locations.

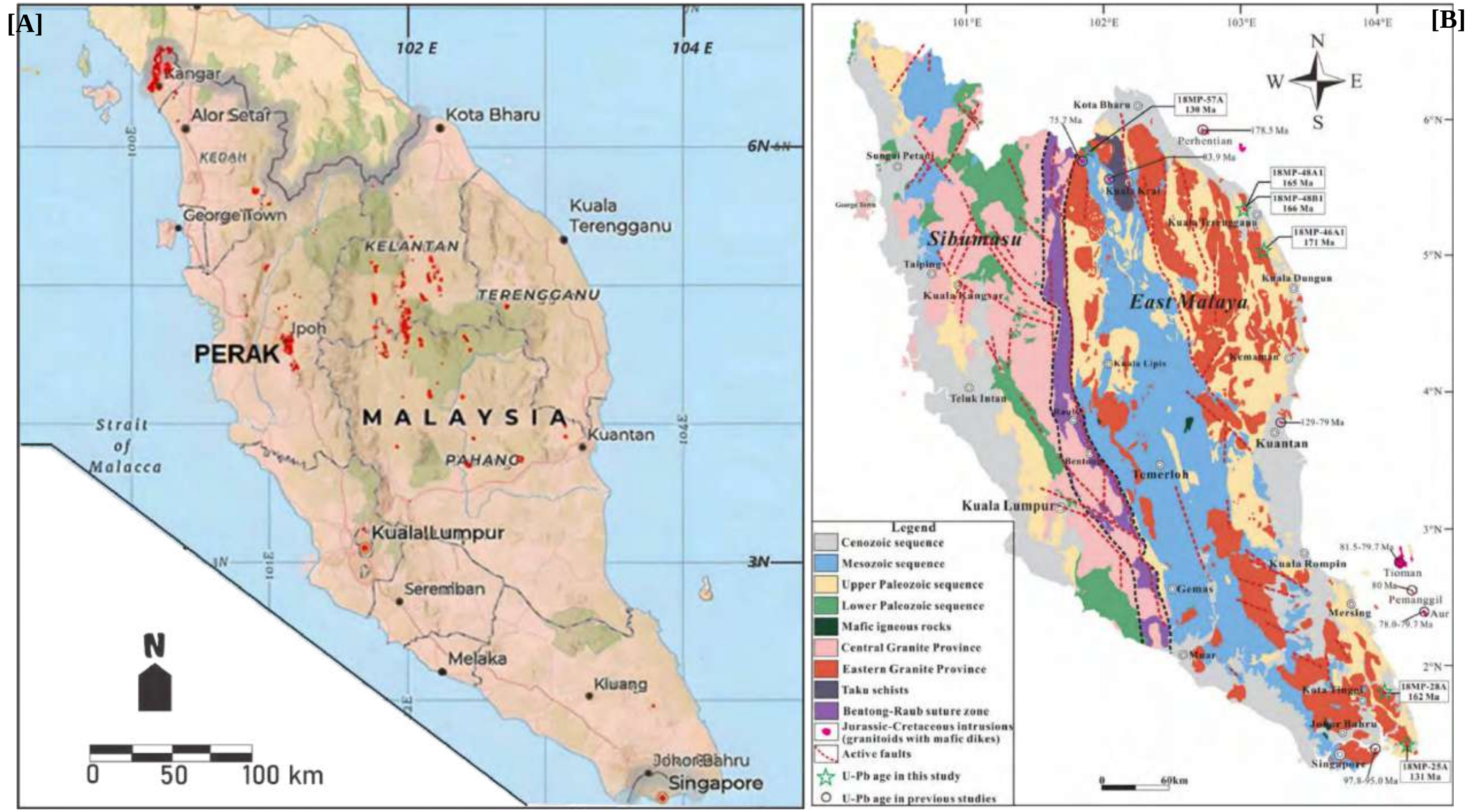

Figure 2. [A] Distribution of carbonate rock outcrops across Peninsular Malaysia (Tan et al., 2024). [B] Tectonic setting of Peninsular Malaysia, showing the three main tectonic belts along with lithostratigraphic units of igneous and sedimentary rocks, modified from Qian et al. (2023), Yu et al. (2022).

MATERIAL AND METHOD

Limestone preparation and Classification

10 limestones unit were cut, grind and polished to form a thin section according to the method Williams et al. (1982). the limestone then observed under the polarizing microscope to microscopic purpose. The limestone was classified in this study require grain support as proposed by Dunham classification (Wright, 1992). The categorization separates carbonate rocks into two major categories: those whose initial components were created in place and consist of intergrowths of skeletal material, and those whose original components were linked together following deposition. This limestone classification will further use for being analysed their porosity using image processing software, which is ImageJ. From this various type of limestone can yield different porosity result.

Software Processing

The programmes ImageJ (ImageJ) will be used to process the images and determine the total porosity and the total number of pores. As a percentage, the image total porosity will be determined by dividing the whole area of the eld by the sum of the areas of all the pores (Cooper et al., 2005). ImageJ is a widely used open-source software for image processing and analysis in various scientific fields, including geology. ImageJ provides tools for enhancing image quality, allowing adjustments to brightness, contrast, and color. Filters for noise reduction, sharpening, and smoothing can also be applied to improve clarity. The software enables measurement of different parameters within an image, including lengths, angles, and areas, through the use of tools such as the line and angle tools, or by selecting regions of interest (ROIs). For accurate measurements, calibration with known reference values is possible. Segmentation techniques facilitate the separation of items from the background, aiding in the identification and quantification of specific features. ImageJ includes a range of analytical methods for data extraction, such as particle analysis for counting objects and texture analysis for evaluating surface characteristics.

Identify Porosity using Image-J.

To identify porosity using ImageJ software, the following method was employed according to Grove and Jerram (2011). First, a high-resolution image of the geological sample, such as a thin section or rock surface, was imported into the software. The scale was adjusted from pixels to micrometers using the ‘set scale’ tool. The image type was changed to 8-bit, and a thresholding technique was applied to determine the sample's porosity. This process converts the image into a binary format, with porosity shown as a red region. Next, the ‘analyze particles’ tool was utilized to calculate the average particle size. These steps were repeated for

BALTICA Volume 37 Number 12 December 2024: 80–99
https://doi.org/10.59879/tWHTQ

each sample. Prior to porosity analysis, it may be necessary to preprocess the image to enhance features and ensure accurate measurements. Techniques such as adjusting brightness and contrast, noise reduction, and filtering can be employed. Thresholding is a key step that separates pores from the background. The image is transformed into a binary format, with pores shown in white and the background in black. ImageJ offers options for manual thresholding, global thresholding (like Otsu or Huang), and adaptive thresholding. The most appropriate method should be chosen based on the image characteristics. Once thresholded, porosity can be calculated using the formula:

Porosity (%) = (Total pore area Total image area) × 100 Porosity (%) = (Total image area Total pore area) ×100

ImageJ includes measurement tools to assess areas and perform calculations. The total pore area can be measured with selection tools, and the total image area can be obtained similarly. To find the porosity percentage, the pore area is divided by the image area and multiplied by 100. It is essential to validate the results by visually inspecting the thresholder image to ensure all pores are accurately captured without extraneous features. If needed, threshold values can be adjusted, and the porosity calculations repeated. ImageJ also offers statistical analysis functions to assist with porosity evaluation, allowing for the computation of pore size distributions and spatial trend analysis.

RESULT AND DISCUSSION

Limestone Classification and Porosity Identification

The Bewah Limestone typically forms in marine environments, suggesting facies variations that include fossil and bioclastic materials deposited during sedimentation. This setting likely corresponds to a shallow marine area influenced by dynamic mean sea levels, ranging from intertidal to lower shoreface zones. In this study, various limestone facies were identified, including mudstone, wackestone, packstone, and rudstone. Mudstone is characterized by less than 5% allochem (i.e., grains smaller than 5 mm) and predominantly consists of lime mud (Figure 3A). The allochem in mudstone includes rare foraminifera and ooids embedded in micrite. Wackestone, on the other hand, contains more than 10% allochem, all less than 5 mm in size and coated in lime mud (Figure 3B). The allochems in wackestone include foraminifera, mollusks, bryozoans, and crinoids. Packstone, in contrast, has a higher allochem content (50-60%), is well-sorted, and is sometimes surrounded by sparite (lime cement) (Figure 3C). Rudstone is characterized by larger grains, typically greater than 5 mm, and sometimes up to 1 cm in size (Figure 3D). It contains abundant foraminifera and mollusks, bonded by sparite and occasionally moderately sorted.

BALTICA Volume 37 Number 12 December 2024: 80–99
https://doi.org/10.59879/tWHTQ

Understanding the sedimentary history and depositional environment of the Bewah Limestone is key to assessing its geological significance and potential as a hydrocarbon reservoir. Thin-section analysis, combined with image-analysis software, allows for accurate determination and calculation of porosity values in rock samples. Porosity, which measures the void spaces or pores within a rock, is an important indicator of fluid storage and flow capacity. Limestones often exhibit a wide range of porosity levels, influenced by their diagenetic and depositional history. Factors such as the initial depositional environment, compaction, cementation, and dissolution all impact porosity (Zhu et al., 2020).

Results from ten limestone samples analyzed using ImageJ software show varying porosity values (see Table 1). Sample LM01 recorded the highest porosity at 20.24%, indicating good reservoir quality with interconnected void spaces that enhance storage capacity and fluid flow, which are favorable characteristics for hydrocarbon storage (Table 1). The grain composition of LM01 likely plays a key role in its high porosity, possibly due to prolonged dissolution processes, influenced by the rock being submerged in lake water. Since the Bewah Limestone area is partly surrounded by water bodies, this may facilitate the dissolution of the rock despite its metamorphosed state, especially given its high bioclast content.

Three samples—LM04 (11.6%), LM08 (14.12%), and LM10 (11.93%)—exhibit fair porosity values (Table 1). These samples contain numerous grains that could contribute to void spaces, particularly bioclast grains. However, not all grain fragments contribute to pore formation, as some still have interlocking secondary calcite minerals. Rocks with fair porosity typically have a moderate number of interconnected pore spaces, which allow for fluid retention but may limit fluid flow compared to higher-porosity rocks. The remaining samples, including LM02, LM03, LM05, LM06, LM07, and LM09, show poor reservoir quality with porosity values below 10% (Table 1). These lower porosity values suggest limited pore space, likely due to diagenetic processes such as secondary cementation and compaction, often associated with metamorphism during igneous intrusion. These samples contain dense lime mud with few bioclast grains, preventing pore formation, and have undergone significant metamorphism.

To visualize these results, the porosity values for each sample are represented in a spider diagram (Figure 4). This diagram groups the limestone samples according to their porosity index. The mudstone facies, represented by LM06 and LM07, show porosity values between 6.52% and 9.25%, classified as having poor porosity. Similarly, the dolomite facies, represented by LM02 and LM03, have poor porosity values ranging from 7.89% to 10.5%. The wackestone facies, represented by samples LM01 and LM04, show porosity values between 11.6% and 20.24%, with a fair to good porosity index. The packstone facies, represented by LM08, LM09, and LM10, show porosity values between 7.85% and 14.93%, classified as poor to fair. Finally, the rudstone facies, represented by LM05, has a poor porosity index of 6.10%.

BALTICA Volume 37 Number 12 December 2024: 80–99
https://doi.org/10.59879/tWHTQ

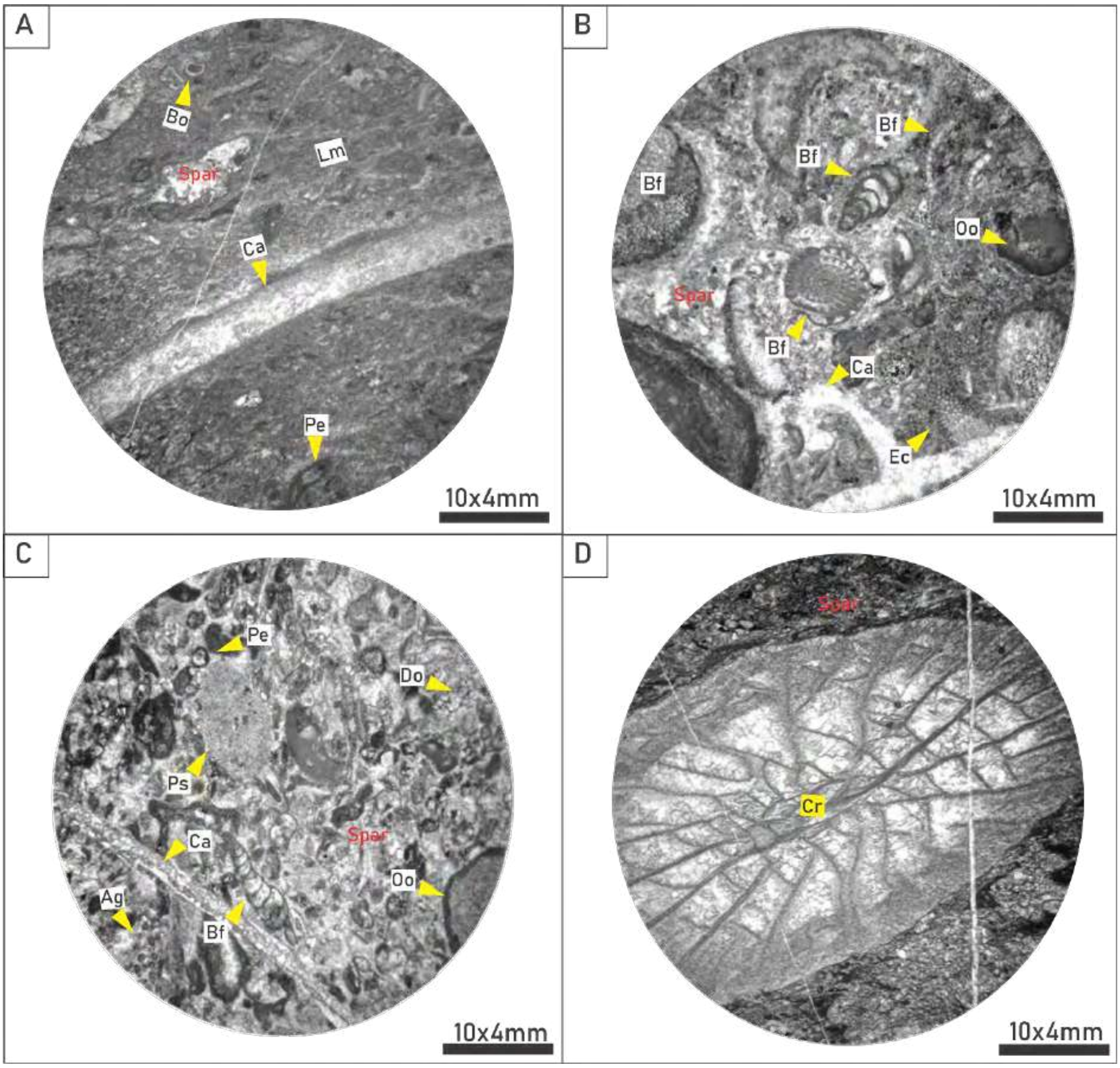

Figure 3. [A] Mudstone sample with a low component of grains, predominantly mud lime. [B] Wackestone sample with various types of grains. [C] Packstone sample with a predominance of grains embedded in micrite-sparite. [D] Rudstone with coral fragments surrounded by sparite. Notes: Bo: Bioclast fragment, Lm: mud lime, Ca: secondary calcite cement, Pe: peloid, Spar: sparite, Bf: benthic foraminifer, Oo: ooid, Ec: echinoderm, Do: dolomite mineral, Ps: pesoid, Ag: algae, Cr: coral.

since 1961
BALTICA Volume 37 Number 12 December 2024: 80–99
https://doi.org/10.59879/tWHTQ

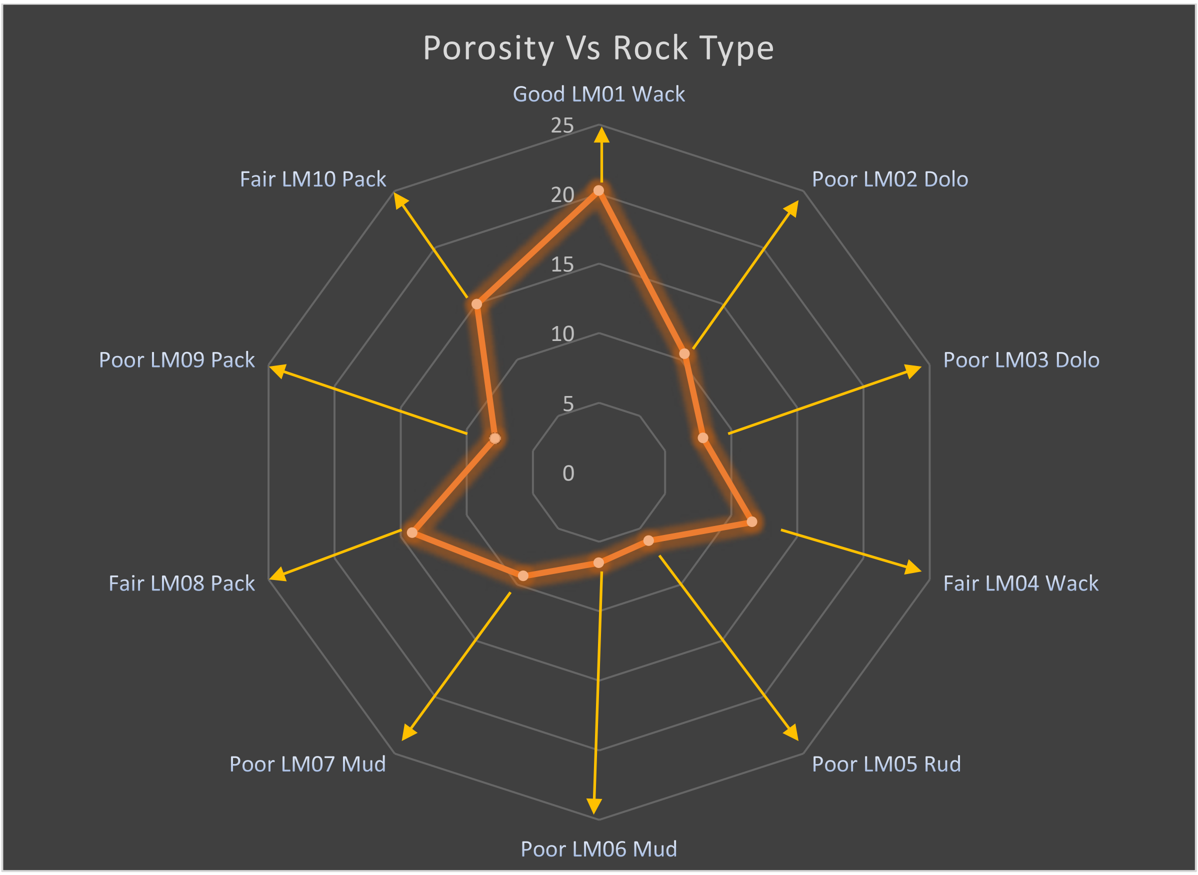

Figure 4. Spider web diagram illustrating a simplified classification of limestone types in relation to porosity values and quality.

BALTICA Volume 37 Number 12 December 2024: 80–99
https://doi.org/10.59879/tWHTQ

Table 1. Simplified limestone classifications, processed images, descriptions, porosity values, and reservoir quality for each sample.

Sample ID	Petrographic image	ImageJ processing	Classification	Description	Porosity ϕ, %	Reservoir quality (Levosen, 1967)
LM01		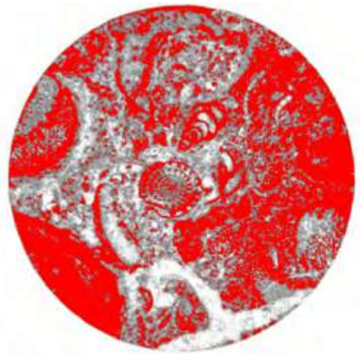	Wackestone	- This sample consists of more than 10% grains embedded in lime mud during deposition. - Various types of grains are present, such as benthic foraminifers, molluscs, and ooidal-peloidal grains. - The processed image shows good porosity due to the preservation of many pores. ImageJ detects numerous greyscale thresholds as surface area.	20.24	Good
LM02		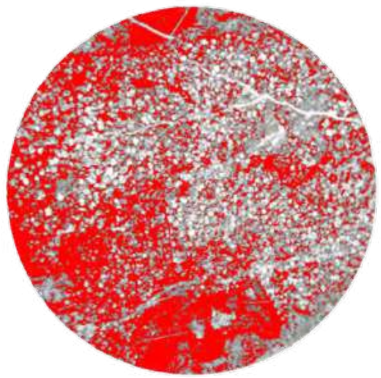	Dolomite	- This sample consists of numerous dolomite minerals formed after deep burial compaction. - The processed image shows poor-quality porosity. - The dolomite includes stylolites as a form of secondary porosity, providing improved pore connectivity; however, their presence is limited.	10.5	Poor

BALTICA Volume 37 Number 12 December 2024: 80–99
https://doi.org/10.59879/tWHTQ

LM03	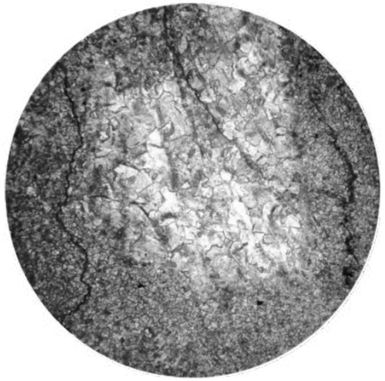	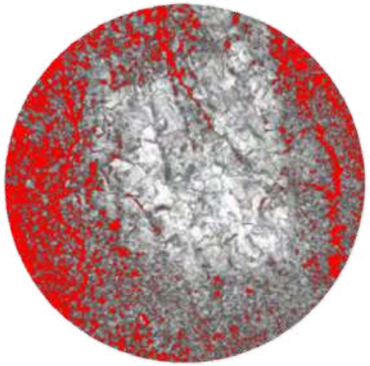	Dolomite	-This sample consists predominantly of dolomite minerals. - The processed image shows poor porosity. - Connective porosity is observed through stylolite thresholding.	7.89	Poor
LM04	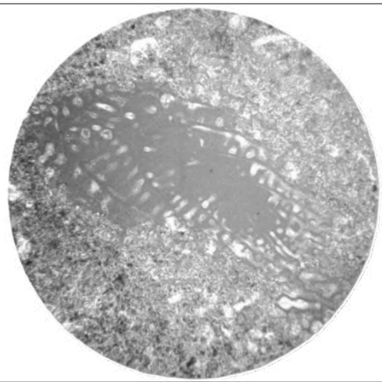	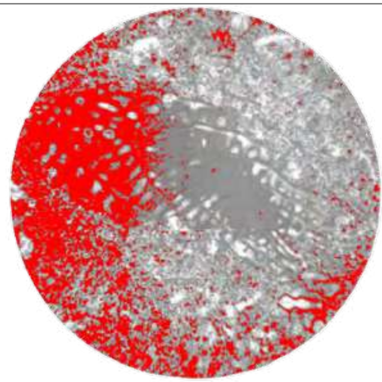	Wackestone	- This sample consists of over 10% grains, predominantly in lime mud, with moderately to poorly sorted grains. - The porosity is fair, and the thresholding area partially detects the shape of benthic foraminifers	11.6	Fair
LM05	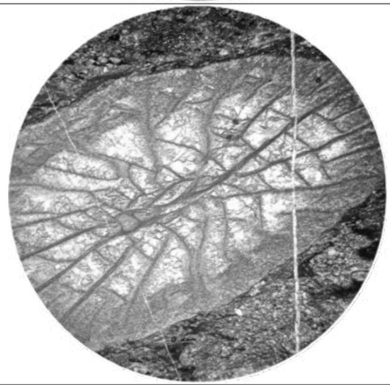	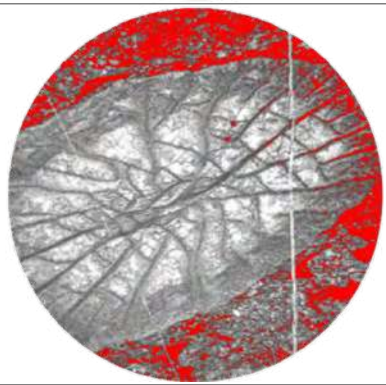	Rudstone	- This sample consists of large, well-sorted grains over 40 mm in size. - The grains primarily consist of coral and some larger molluscs. The porosity is poor, as only micrite-sparite voids are detected. - The coral shows crystalline structure with crystal growth along lineations.	6.10	Poor

BALTICA Volume 37 Number 12 December 2024: 80–99
https://doi.org/10.59879/tWHTQ

LM06		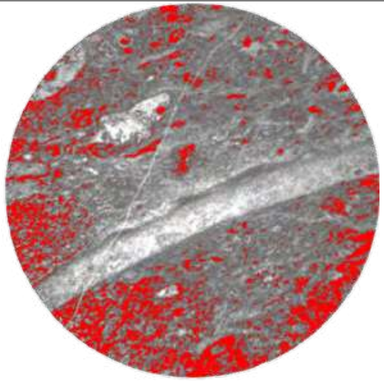	Mudstone	- This sample is predominantly lime mud with minimal grain presence, containing less than 5% grains overall. - The porosity is isolated and of poor quality, with limited exposure in the thin section. Software analysis shows only a low threshold detection.	6.52	Poor
LM07		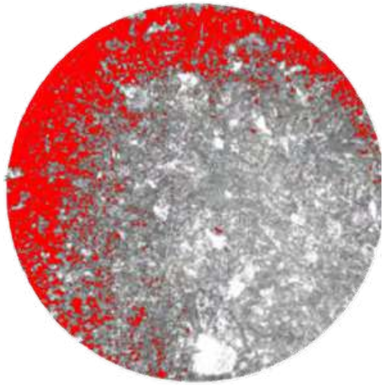	Mudstone	- This sample contains few grains and is predominantly lime mud, most of which is crystallized. The sample primarily consists of calcite minerals. - The processed image shows poor porosity due to low threshold detection, likely because most areas are crystallized.	9.25	Poor
LM08	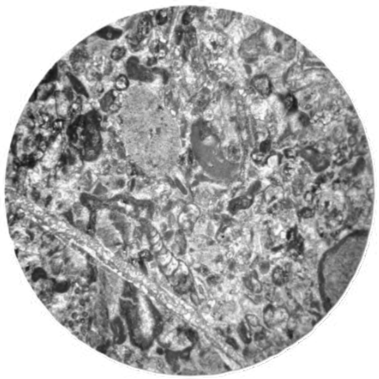	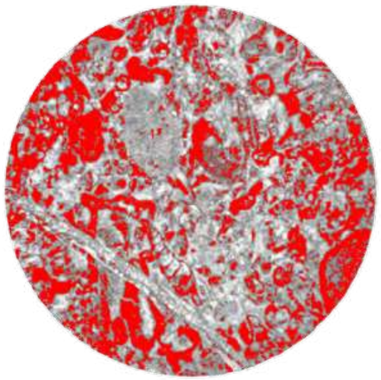	Packstone	- This sample is characterized by having more than 10% grains with less lime mud. - The grains are moderately sorted, consisting mainly of benthic foraminifers and ooidal-peloidal grains. - The processed image shows fair porosity quality. The thresholding area is ideal for detecting porosity, especially in the bioclastic grains.	14.12	Fair

BALTICA Volume 37 Number 12 December 2024: 80–99
https://doi.org/10.59879/tWHTQ

LM09		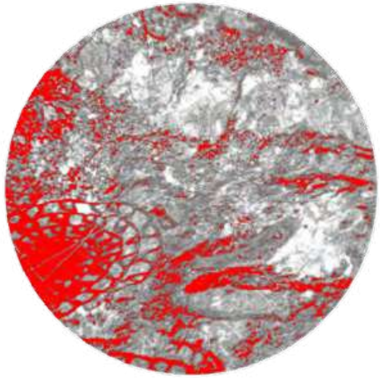	Packstone	- This sample consists predominantly of grains (>10%) and contains less lime mud. - The grains mainly include benthic foraminifers, crinoids, algae, and ooidal-peloidal grains. Micrite and sparite surround the grains. - This sample also shows numerous secondary cements. - The processed image indicates poor porosity, which is due to a lack of voids, as they are largely closed due to diagenetic events.	7.85	Poor
LM10		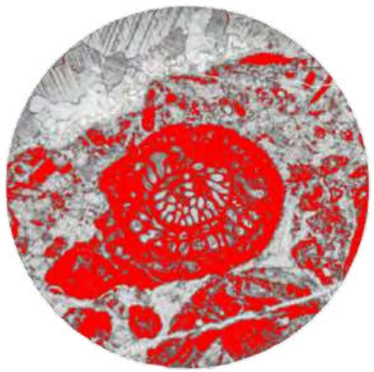	Packstone	- This sample is similar to LM09, as it consists of dominant grains and less lime mud. - The grains are largely composed of benthic foraminifers and algae. Secondary cement is clearly visible in the sample and appears crystalline. - The processed image indicates fair porosity quality. Compared to LM09, bioclastic grains like benthic foraminifers contribute more to productive porosity, and the area is less influenced by diagenetic events.	14.93	Fair

Implications for Suitability as a Reservoir Analogue

Porosity analysis using ImageJ software demonstrates its ability to quantitatively assess porosity in Permian limestone samples. However, comparing these results with traditional core analysis methods, such as poro-perm analysis, is essential to confirm the exact porosity values. Since this study focuses on Permian-age limestone, it is important to note that metamorphism in certain areas of the rock may result in reduced porosity and lower reservoir quality. While porosity varies across the limestone samples, suggesting potential for hydrocarbon storage, the poor connectivity between pores limits its overall effectiveness. Some samples, however, exhibit good pore connectivity. The Permian limestone in Malaysia has undergone varying degrees of metamorphism, which has led to significant compaction and crystallinity, generally preventing hydrocarbon entrapment, particularly in subsurface limestone sequences (Table 1, see LM02-LM03). In contrast, outcrop limestone is more exposed to climatic variations and intense weathering, whether from rainfall or submersion in bodies of water like lakes or oceans, which helps create pore spaces. This study is most relevant to sedimentary rock that has not undergone significant metamorphism and retains primary porosity—whether intra- or intergranular—due to dissolution processes. Additionally, certain areas of the Bewah Limestone may not have experienced substantial tectonic activity, which could have preserved its original primary porosity, as suggested by the porosity results (see Table 1).

The porosity values estimated with ImageJ software rely on a threshold effect based on grayscale, treating pores as image-based features to assess their surface area (Table 1; Figure 5A and B). This approach corresponds well with the limestone samples, which mainly show low porosity values for mudstone, dolomite, and wackestone. Pore connectivity can be further analyzed by applying different colors for thresholding and segmentation (Pal et al., 2022), enhancing the ability to identify porosity. Isolated and unconnected pores are common, where voids appear detached or as separate features (Figure 5A and B). This type of porosity likely results from pore enlargement during dissolution processes that occur after compaction, particularly during deep burial diagenesis (Ali et al., 2006). Effective (or continuous) porosity becomes visible with an alternate threshold (Figure 5B), which reveals connected pores that enable fluid flow through continuous pathways, provided there is clear pore connectivity. This is particularly evident in samples with more bioclastic grains (Figure 5C). Bioclastic grains, especially fossil fragments, help create better pore spaces after dissolution. This process is particularly important in metamorphic rocks, where dissolution occurs after secondary sparite has embedded in the pores. The dissolution agents in this case come from long-term interactions with water that attract minerals. Pore connectivity in limestone is often represented by stylolites, which can be either micro- or macro-scale features formed during pressure dissolution after compaction. The continuous nature of stylolites, similar to seismic reflections, can enhance pore connectivity in the rock, with their amplitude and morphology having a direct impact on reservoir quality (Nikbin et al., 2024). This connected porosity is especially crucial for secondary pores created in metamorphosed rock.

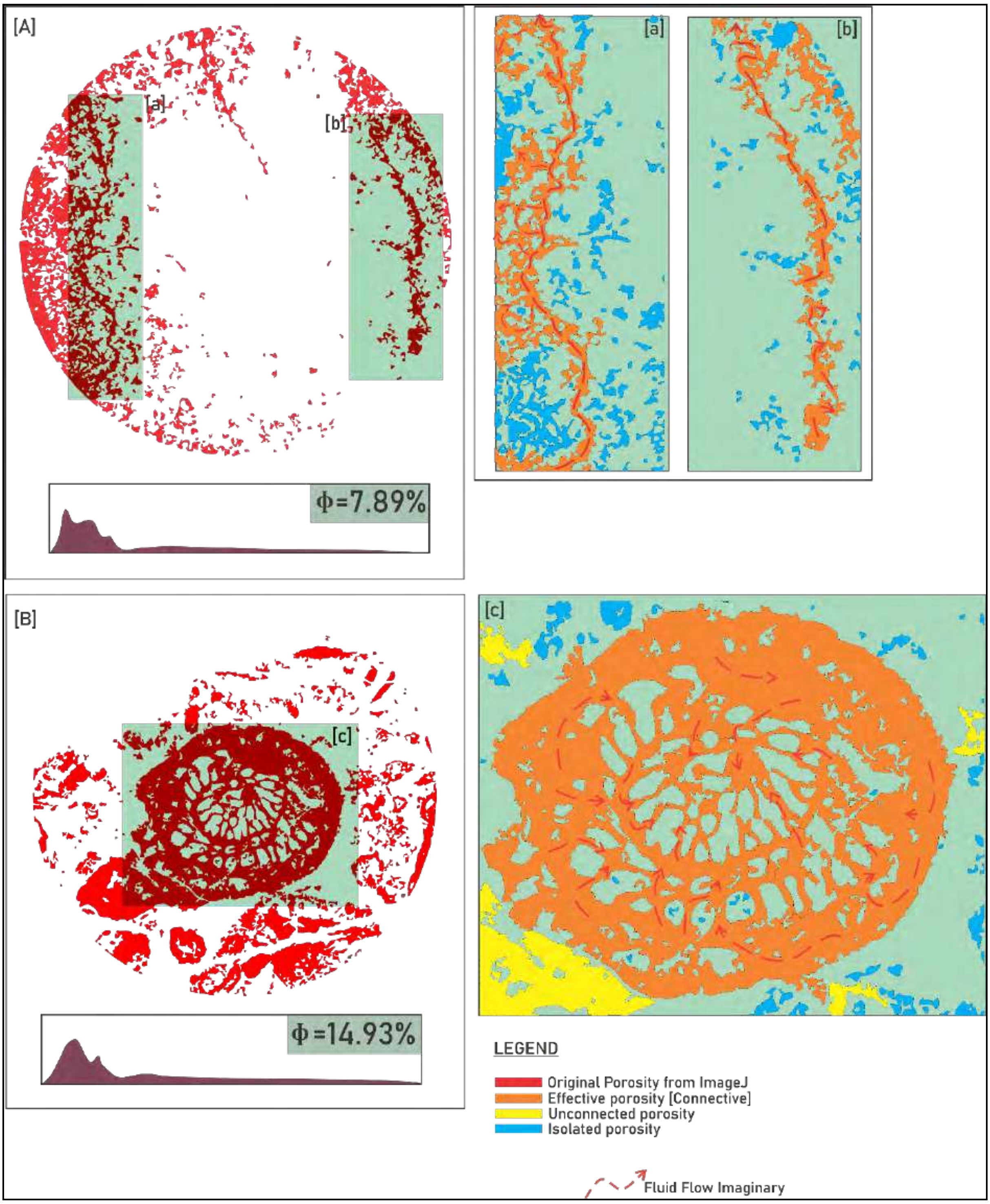

Figure 5. (A) Pore segmentation from the thin section processed with ImageJ, showing a porosity value of 7.89%, which indicates poor quality. (a) and (b) Different thresholding

techniques using various colors demonstrate the identification of isolated, unconnected, and connected porosity. (B) Another image segmentation of packstone yielded a porosity of 14.93%, indicating fair quality. (c) This shows connected porosity in the bioclastic grains after applying different thresholds. Note that the imaginary fluid flow is also used to explain fluid movement in the connected porosity.

CONCLUSIONS

This study concludes that the Bewah Limestone can be classified into mudstone, wackestone, packstone, and rudstone, with each facies exhibiting distinct characteristics, including grain size, mud content, and the degree of diagenesis. Mudstone and wackestone are primarily composed of lime mud with poorly sorted grains, while packstone contains a higher proportion of grains, less lime mud, and moderately sorted particles. Rudstone, in contrast, consists of larger, moderately to well-sorted grains. Each limestone type also displays varying porosity values, ranging from poor to good, based on hydrocarbon reservoir quality indices. However, many samples show low porosity, suggesting that the hydrocarbon reservoir quality may be suboptimal. Despite the generally low hydrocarbon potential due to deep burial diagenesis and tectonic influences, image processing using various threshold and segmentation techniques reveals areas with effective porosity, where connected pores are capable of trapping or conducting hydrocarbon fluids. On a microscale, this study suggests that Bewah Limestone has potential as a hydrocarbon reservoir analogue, though it may not be suitable for commercial exploitation due to the low porosity and permeability observed in many samples. Finally, it is important to emphasize that porosity alone does not fully determine a rock’s suitability as a reservoir. Other factors, such as permeability, mineralogy, and the diagenetic history, also play crucial roles in assessing the rock’s capacity for fluid storage and flow, impacting its suitability for various applications.

ACKNOWLEDGEMENTS

We would like to extend our heartfelt gratitude to Universiti Malaysia Terengganu for funding this research. This research was supported by the Talent and Publication Enhancement Research Grant (TAPE-RG) 2020 (Vot Number: 55258).

REFERENCES

Ali, C. A., Leman, M. S., Mohamed, K. R. 2004. Fasies karbonat dan diagenesis di dalam batu kapur Bukit Biwah dan Bukit Taat, Kenyir, Ulu Terengganu, Bulletin of the Geological Society of Malaysia, 49: 61-65.

Beggan, C., & Hamilton, C. 2010. New image processing software for analyzing object size-frequency distributions, geometry, orientation, and spatial distribution. *Computers & Geosciences*, 36 (4), 539–549.

Chung, K. W., Leman, M. S., Dzulkafli, M. A.,Mohamed, K. R., Ali, C. A., Talib, J.A. 2017. Sedimentologi Batuan Enapan Daratan Kumpulan Gagau (Usia KapurAwal) di Hulu Sungai Chichir, Terengganu Darul Iman, Malaysia. Sains Malaysiana, 46 (12): 2315-2323.

Cooper, M., Vidal-Torrado, P., Chaplot, V. 2005. Origin of microaggregates in soils with ferralic horizons. *Scientia Agricola*, *62*(3): 256-263

Grove, C., & Jerram, D. A. 2011. JPOR: An ImageJ macro to quantify total optical porosity from blue-stained thin sections. *Computers and Geosciences*, *37*(11): 1850-1859

Hersum,T.G & Marsh,B.D.2007. Igneous textures: on the kinetics behind the words. Elements, 3:247–252

Higgins, M.D. & Roberge, J. 2007. Three magmatic components in the 1793 eruption of Eldfell volcano, Iceland: evidence from plagioclase crystal size distribution (CSD) and geochemistry. *Journal of Volcanology and Geothermal Research*, 161: 247–260.

Janjuhah, H. T., Kontakiotis, G., Wahid, A., Khan, D. M., Zarkogiannis, S. D., Antonarakou, A. 2021. Integrated porosity classification and quantification scheme for enhanced carbonate reservoir quality: Implications from the miocene malaysian carbonates. *Journal of Marine Science and Engineering*, *9*(12).

Jerram, D.A. & Cheadle, M.J. 2000. On the cluster analysis of rocks. *American Mineralogist* 85: 47–67.

Jerram, D.A. 2001. Visual comparators for degree of sorting in 2-D and 3-D. *Computers & Geosciences*, 27, 485–492

Jerram, D.A., Mock, A., Davis, G.R., Field, M., Brown, R.J. 2009. 3D crystal size distributions: a case study on quantifying olivine populations in kimberlites. *Lithos* 112S: 223–235

Khoo, T.T., & Tan, B.K. 1983. Geologic evolution of Peninsular Malaysia. *Newslett Geol Soc Malays*, 2(5):234

Levorsen, A.I. (1967) Geology of Petroleum. 2nd Edition, W. H. Freeman and Company, San Francisco, CA.

Machel, H.G. 2005. Investigations of Burial Diagenesis in Carbonate Hydrocarbon Reservoir Rocks. Geoscience Canada, 32: 103-128.

Metcalfe, I.1988. Origin and assembly of Southeast Asiancontinental terranes. In: Audley-Charles MG, Hallam A(eds) Gondwana and Tethys. Geological Society, vol37, London, Special Publications, pp 101–118.

Metcalfe, I. 2011. Palaeozoic–Mesozoic history of SE Asia. The Geological Society of London, (355), 7-35.

Morton-Thompson, D., & Woods, A. M. 1993. Development geology reference manual. *Development Geology Reference Manual*. 550 p.

Mustaffa, K.S. 2009. Major Faults. In: Hutchison, C. S., & Tan, D. N. K. (eds). Geology of Peninsular Malaysia. University of Malaya/Geological society of Malaysia, Kuala Lumpur, 249-269.

Nguyen Hoang Viet, N.H. 2014. Sedimentological and Petrophysical Properties of Sandstone Facies belonging to Lambir Formation at Tusan Beach, Miri, Sarawak. Thesis, unpublished. 55 p.

Nikbin, M., Moussavi-Harami, R., Moghaddas, N. H., Aghli, G., Ghaemi, F., & Aminshahidy, B. 2024. The role of stylolites as a fluid conductive, in the heterogeneous carbonate reservoirs. *Journal of Petroleum Exploration and Production Technology*.

Pal, A. K., Garia, S., Ravi, K., Nair, A. M. 2022. Pore scale image analysis for petrophysical modelling. *Micron*, 154: 1-16

Qian, X., Bai, T., Yu, Y., Mustapha, K. A., Sheldrick, T. C., Gan, C., & Wang, Y. (2023). Multiple stages of continental rifting in Eastern Peninsular Malaysia: new insights from Jurassic–Cretaceous granitoids. *Journal of the Geological Society*, *180*(5).

Rahman, M.N.I.A., Roslan, A.N., wali, S.S.A.S., Baharim, N.B., Ghani, A.A, Ali, C.A. 2023. Petrographic features and modelling of some waterfall rocks in kenyir lake, terengganu: a microscopic perspective approach in sustainable geotourism, *Journal of Sustainability Science and Management*, 18 (2): 51-66.

Rine, J. M., Smart, E., Dorsey, W., Hooghan, K., Dixon, M. 2013. Comparison of porosity distribution within selected North American shale units by SEM examination of argon-ion-milled samples. In *AAPG Memoir*, 102: 137-152

Roselee, M. H., Umor, M. R., Ghani, A.A., Badruldin, M. H., Quek, L. X. 2018. Petrographic and geochemical characteristic of volcanic rocks fromTasik Kenyir and Kampung Awah, EastMalaya block, Peninsular Malaysia. AIP Conference Proceedings. 1940, 020033.

Baltica

BALTICA Volume 37 Number 12 December 2024: 80–99
https://doi.org/10.59879/tWHTQ

Saraf, S., Singh, A., Desai, B. G. 2019. Estimation of Porosity and Pore size distribution from Scanning Electron Microscope image data of Shale samples: A case study on Jhuran formation of Kachchh Basin, India. *Exploration Geophysics*, 1: 1-3

Sharoum, F. M., Abdullah, M. T., Ali, C. A., & Ismail, R. 2015. Geopark Tasik Kenyir. Universiti Malaysia Terengganu, pp. 104.

Stevens, L. 2016. Reservoir analysis of the compartmentalized Mississippian ages Spivey-Grabs field, south central Kansas, Thesis unpublished. 69 p

Tan, J.P.C., Kiew, R., Darbyshire, I. 2024. Prioritising Important Plant Areas (IPAs) among the limestone karsts of Perak, Malaysia, *Kew Bulletin*, 79(2):1-19

Williams, H., Turner, F. J., Gilbert, C. M. (1982). Petrography: an introduction to the study of rocks in thin sections. *Petrography: An Introduction to the Study of Rocks in Thin.*

Wright, V. P. (1992). A revised classification of limestones. *Sedimentary Geology*, *76*: 3–4.

Xia, L. W., Cao, J., Wang, M., Mi, J. L., Wang, T. T. 2019. A review of carbonates as hydrocarbon source rocks: basic geochemistry and oil–gas generation. In *Petroleum Science*, 16 (4).

Yu, Y., Qian, X., Azlan Mustapha, K., Sheldrick, T. C., Gan, C., Zhang, Y., Wang, Y. 2022. Late Paleozoic–Early Mesozoic granitic rocks in Eastern Peninsular Malaysia: New insights for the subduction and evolution of the Paleo-Tethys. *Journal of Asian Earth Sciences*, *239*:1-17.

Zahidin, M.A., Omar, W.B.W., Taib, W.R.W., Ryan, J.J.R., Harun, A., Abdullah, M.T. 2017. Ethno-Tourism: The Historical and Cultural Exploration of Gua Bewah in Tasik Kenyir, Terengganu. In: Ecotourism Potentials in Malaysia. UPM, pp. 96-102.

Zhu, X., Jin, Z., Liang, T., Yi, S., Wei, K., Gao, B., Shi, L. 2020. Depositional environment, diagenetic evolution, and their impact on the reservoir quality of the carboniferous KT-Ⅱ carbonate in the zhanazhol reservoir, Pre-Caspian Basin, Kazakhstan. *Marine and Petroleum Geology*, *117*. 104411